Trans Indian Inst Met (2024) 77(9):2471–2478
https://doi.org/10.1007/s12666-024-03333-9

ORIGINAL ARTICLE

Processing and Properties of Ultra-Fine Quaternary Cu-Based Pre-alloyed Powder for Diamond Tools by Co-precipitation Process

Changjiang Xiao[1] · Lihui Tang[1] · Qunfei Zhang[1] · Haoyu Zheng[1]

Received: 3 December 2023 / Accepted: 10 April 2024 / Published online: 7 May 2024

Abstract In this paper, the preparation of pre-alloyed powder and its effect on the properties of metal-bonded diamond tools were systematically studied. A co-precipitation process was used to prepare ultra-fine quaternary Cu-based pre-alloyed powder. The optimal parameters of preparing the precursor powder were precipitation temperature of 50 ℃ and reactant concentration of 1 mol/L. After the precursor powder was calcined and reduced by hydrogen, ultra-fine Cu-based pre-alloyed powder with an average particle size of about 0.55 μm was obtained and its main components were Cu, Fe, Ni, Cu–Sn, and Fe_3Ni_2. Furthermore, the mechanical properties of the bulks with pre-alloyed powders and the elemental metal powder mixture of equivalent composition were investigated. The results demonstrated that the mechanical properties of sintered bulks, including relative density, hardness and flexural strength, were improved using pre-alloyed powder. The optimal hardness and flexural strength values of the bulks with pre-alloyed powder were 110 HRB and 1056 MPa, respectively, which were 10.0% and 24.8% higher than those of the mixed powder matrix (100 HRB and 846 MPa). With the addition of diamond particles, the maximum flexural strength of the bulks reduced to 882 MPa, which was still 24.1% higher compared to the mixed powder matrix (711 MPa). In addition, the cutting ability of the diamond saw blade with pre-alloyed powder was superior to that with the elemental metal mechanical mixing powder.

Keywords Cu-based pre-alloyed powder · Diamond tool · Co-precipitation process · Microstructure · Mechanical property

1 Introduction

The most commonly used metal matrix for diamond-sintered tools is the elemental metal mechanical mixing (EMMM) powder [1–5]. Although the EMMM powder has the advantage of being able to easily regulate the ratio of each type of metal powder, complete alloying of the matrix is difficult due to component segregation caused by the metal powder. Hence, it is not easy to achieve uniform mixing, which then affects the properties of diamond tools. In recent years, researchers have developed new materials to replace metal mixtures and solve the above problems. As each particle of pre-alloyed (PA) powder contains the entire composition, the sintering temperature can be decreased by using PA powder. More importantly, problems with EMMM powders such as uneven component distribution and diamond heat deterioration are effectively resolved by PA powders.

According to literature reports, when diamond tools are sintered by PA powders, their properties are greatly improved [6–11]. Bai et al. [12] reported that PA powder can effectively improve the mechanical properties of matrix. When the content of PA powder increased from 5 to 25%, the bending strength increased from 966 to 1221 MPa. Hu et al. [13] suggested that pre-alloyed Cr-Fe and Fe can completely replace tungsten carbide as the framework material of the matrix. Chu et al. [14] reported that the PA powder prepared by ultra-high-pressure water atomization exhibited the best mechanical properties including relative density, hardness and bending strength of matrix-sintered segment. Moreover, the service life of diamond tools was greatly

✉ Changjiang Xiao
cjxiao@haut.edu.cn

[1] Department of Material Science and Engineering, Henan University of Technology, Zhengzhou 450001, China

improved. Zhao et al. [15] suggested that it is feasible and reasonable to replace Fe elemental powder by Fe-based PA powders to fabricate impregnated diamond bits. Dai et al. [16] found that pre-alloying can improve homogeneity of alloy element distribution in the matrix and increase the hardness and strength. Xu et al. [17] reported that diamond wire saw prepared by a novel water-atomized PA powder achieved a satisfactory result for cutting natural hard granite. Additionally, the pre-alloying technique can shorten sintering times and lower sintering temperatures [5–9] by lowering the activation energy during sintering [5, 15, 16].

The water atomization method [14, 17, 18] and the co-precipitation method [19, 20] are the two most commonly used processes to prepare PA powder for diamond tools. The co-precipitation method can immediately generate powder with a homogenous chemical composition through precipitation reactions, and it allows metal ions to precipitate in the solution simultaneously. Consequently, the co-precipitation method is also frequently used to produce micro- and nanoparticles [21–24], and it is considered to be a promising method for producing PA powder with fine grains and uniform distribution of elements. Some studies on quaternary PA powders [25] and even quinary PA powders [17, 26] have been conducted recently. However, so far, there is little systematic research on the preparation of quaternary PA powder and the properties of diamond bulks sintered using PA powder, especially on Cu-based PA powders.

In this paper, ultra-fine-grained and high-strength quaternary Cu-based PA powder for diamond tool was prepared using $CuCl_2{\cdot}2H_2O$, $FeCl_2{\cdot}4H_2O$, $SnCl_2{\cdot}2H_2O$ and $NiCl_2{\cdot}6H_2O$ as raw materials, and $H_2C_2O_4{\cdot}2H_2O$ as precipitator. Moreover, the bulks were prepared utilizing PA powders and EMMM powders of equal composition by hot-pressing sintering at different temperatures, and their mechanical characteristics were compared. After the addition of diamond particles, the diamond bulks were sintered using the same technique. The holding force between the matrix and diamond was evaluated by measuring the flexural strength of the bulks. The cutting efficiency of the diamond saw blades was also investigated. The flexural morphology of these materials was also examined in order to explain the differences in their properties.

2 Experimental

2.1 Preparation of Cu-Based Pre-alloyed Powder

In the co-precipitation process, each component was weighed out based on the weight percentage indicated in Table 1. Each powder reagent had a purity level of 99.9%. First, raw materials such as $CuCl_2{\cdot}2H_2O$, $FeCl_2{\cdot}4H_2O$, $SnCl_2{\cdot}2H_2O$ and $NiCl_2{\cdot}6H_2O$ were accurately weighed and mixed evenly, and an oxalic acid solution with deionized water was prepared simultaneously. Second, they were mixed in a 1:1 volume ratio, and the co-precipitation process was carried out in the reaction vessel. During the co-precipitation, the water bath was heated to the desired temperature, and the pH value was adjusted with ammonia. Following the reaction, the product was filtered, cleaned and vacuum-dried to obtain the precursor powder. The effects of the co-precipitation factors on the yield and grain size of the precursor powder were researched, and the corresponding process parameters were optimized. After filtering, washing, calcining and reducing the precursor, PA powders were obtained.

Table 1 Composition of Cu-based pre-alloyed powder

Raw materials	$CuCl_2{\cdot}2H_2O$	$FeCl_2{\cdot}4H_2O$	$SnCl_2{\cdot}2H_2O$	$NiCl_2{\cdot}6H_2O$
Weight percent (%)	50	30	10	10

2.2 Sintering of Bulks

To assess the matrix properties, the bulks were sintered using the PA powders. The sintering procedure is described in detail in our earlier report [27]. Then, diamond particles were added and the diamond bulks were sintered under the same parameters. The following are the specifications of the artificial diamond particles (Model MBD-6): 40/50 mesh (380/340 μm) grain size, 40% volume concentration. The sintering temperatures were selected to be 760, 780, 800, 820, 840 and 860 °C. After sintering, the sample surfaces were flattened and polished to evaluate their mechanical properties.

For comparison, EMMM powder of Cu, Fe, Sn and Ni single elements was used as the raw material to prepare Cu-based diamond bulks with the same component. EMMM powders were purchased from Tianjin Kemiou Chemical Reagent Co., China. The sizes of the particles were 74, 67, 54 and 30 μm, respectively.

2.3 Characterization and Testing of Mechanical Properties

The phase composition of the PA powder was analyzed by X-ray diffractometer (XRD; D8 advance, Germany). The morphology, grain size and microstructure were observed by scanning electron microscope (SEM, ZZIS SUPRA-55, Holland). The chemical composition was investigated using energy-dispersive spectroscopy (EDS) coupled to SEM apparatus. Archimedes method was carried out to measure the relative density. An HR-150A Rockwell hardness tester

was used to measure the hardness. The flexural strength of the sintered samples was tested on an INSTRON-5569 tester. At least five measurement results were collected for each sample, and the average value was selected as the representative one.

3 Results and Discussion

3.1 Factors Influencing the Co-precipitation Process

3.1.1 Reaction Temperature

The key factors in the co-precipitation process are the reaction temperature and reactant concentration. The effect of reaction temperature on grain size and yield of the precursor powder is illustrated in Fig. 1. As the reaction temperature increases, the grain size of the precursor first decreases and then increases, while the yield of the precursor shows the opposite trend. When the temperature is 50 °C, the grain size of the precursor is about 1.54 μm which is the finest particle size, and the precursor yield reaches 92.8%. Combining the two aspects of particle size and yield of powder, the suitable precipitation temperature is selected as 50 °C.

When the temperature is below 50 °C, the rate of co-precipitation increases. As a result, the rate of nucleation increases as well, resulting in smaller particle sizes and higher powder yield [28]. When the temperature exceeds 50 °C, the grain growth rate exceeds the nucleation rate, resulting in larger grains. Furthermore, the super-saturation of the solution decreases and the formation of unstable grains increases at temperatures above 70 °C, which lowers the precursor powder yield. As a result, at 50 °C, the precursor powder has the lowest grain size and the highest yield.

3.1.2 Reactant Concentration

Figure 2 shows the influence of reactant concentration on particle size and powder yield of the precursor. Similarly, there is a decreasing and subsequently increasing relationship between particle size and reaction concentration. When the initial reactant concentration is 0.4 mol/L, the grain size is 2.28 μm. As the reactant concentration increases to 0.6 mol/L, the grain size increases to a maximum value of 3.86 μm. Then, the grain size steadily decreases to a minimum value of 1.14 μm as the reactant concentration rises to 1 mol/L. The grain size keeps increasing as the reactant concentration rises. On the other hand, when the reactant concentration is increased, the powder yield improves.

The yield of powder improves from 35.6% to 98.8% as the solution concentration increases from 0.4 to 1.2 mol/L. Based on the described experimental findings, 1.0 mol/L is selected as the optimal reactant concentration. The ideal reactant concentration and reaction temperature are the same for the Fe-Cu-Co-based PA powder made using this technique [19].

3.2 Phase Composition and Morphology of Pre-alloyed Powder

After calcining the precursor powder at 500 ℃ and then reducing it with hydrogen, Cu-based PA powder is obtained. In order to determine the phase composition of as-prepared PA powder, its XRD pattern is shown in Fig. 3. The sharp diffraction peaks show that the powder has good crystallinity. Comparison with the standard PDF cards indicates that the main components of the PA powder are Cu, Fe, Ni, Cu–Sn and Fe_3Ni_2. These results suggest that Ni and Sn

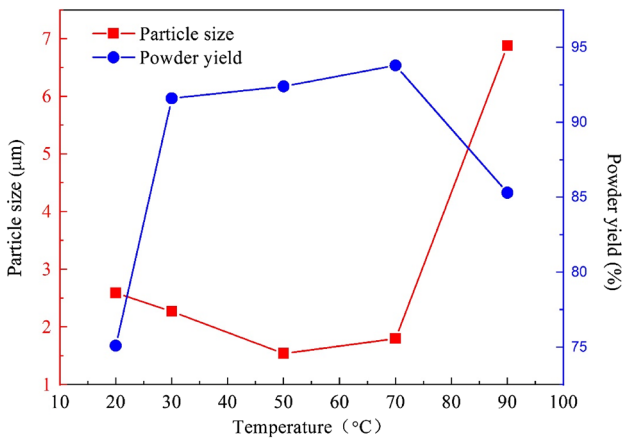

Fig. 1 Effect of reaction temperature on grain size and yield of the precursor powder

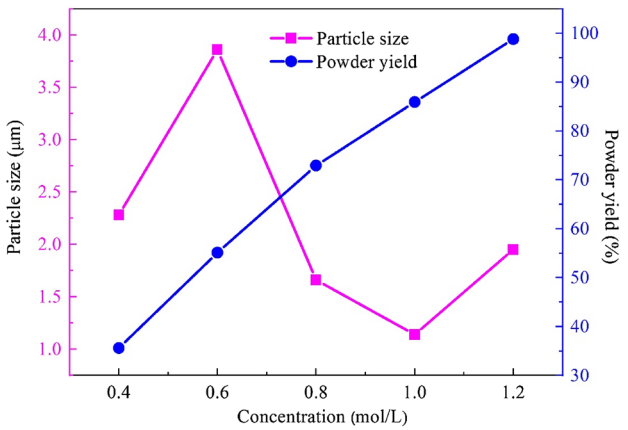

Fig. 2 Effect of reactant concentration on grain size and yield of the precursor powder

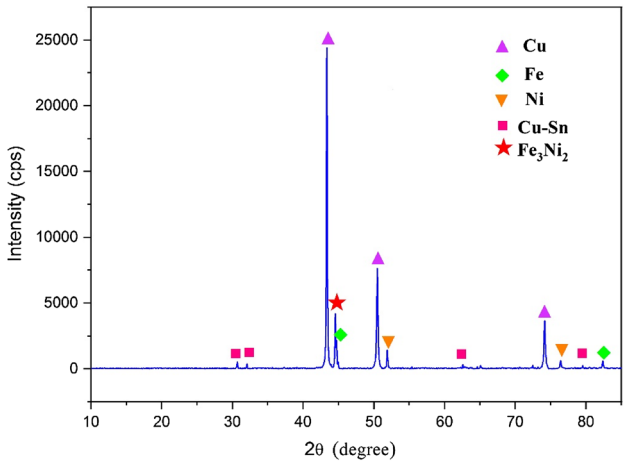

Fig. 3 XRD pattern of Cu-based pre-alloyed powder

atoms interact with Fe and Cu structures, respectively, to generate solid solutions.

Figure 4 shows a SEM image of freshly made PA powder. The powder has uniform grain size and is made up of small particles that are linked, with an average diameter of approximately 0.55 µm (refer to the inset in Fig. 4). Compared to ternary Cu–Fe–Co (16.98 µm) generated using ultra-high-pressure water atomization and ordinary water atomization (34.56 µm), its grain size is significantly reduced [14]. Additionally, it is smaller than the co-precipitation method-prepared Fe–Cu–Co-based PA powder (3 µm) [19]. Furthermore, the powder's surface is loose, and the majority of the particles have irregular morphology. A small degree of agglomeration is present, but it is hardly noticeable.

EDS tests were carried out on the area designated in Fig. 4 (the intersection of two red lines) to further identify the composition of as-prepared PA powder, and the analysis results are shown in Fig. 5. Only five elements are detected: Cu, Fe, Ni, Sn and O, with the relative mass fractions of 51.09%, 28.03%, 9.83%, 9.45% and 1.08%. The above results show that the composition of the PA powder is identical to that of the raw components.

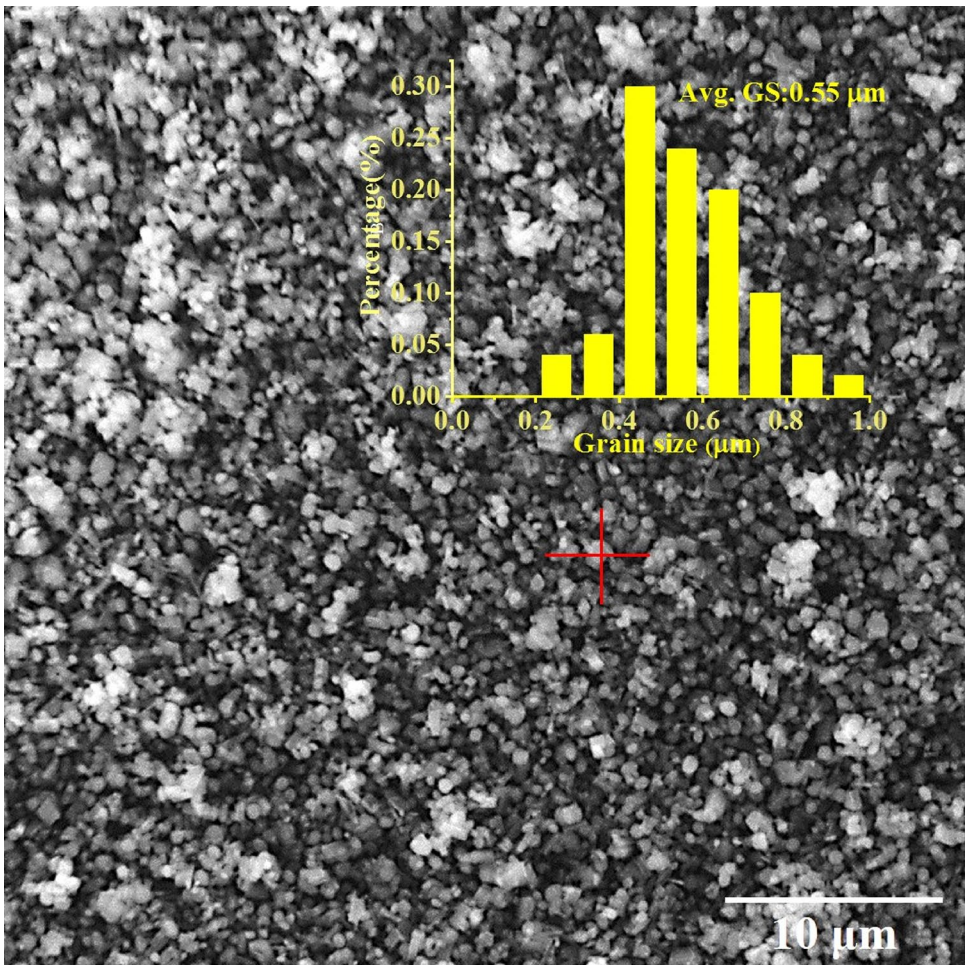

Fig. 4 SEM image of Cu-based pre-alloyed powder, the inset represents the grain size distribution of pre-alloyed powder

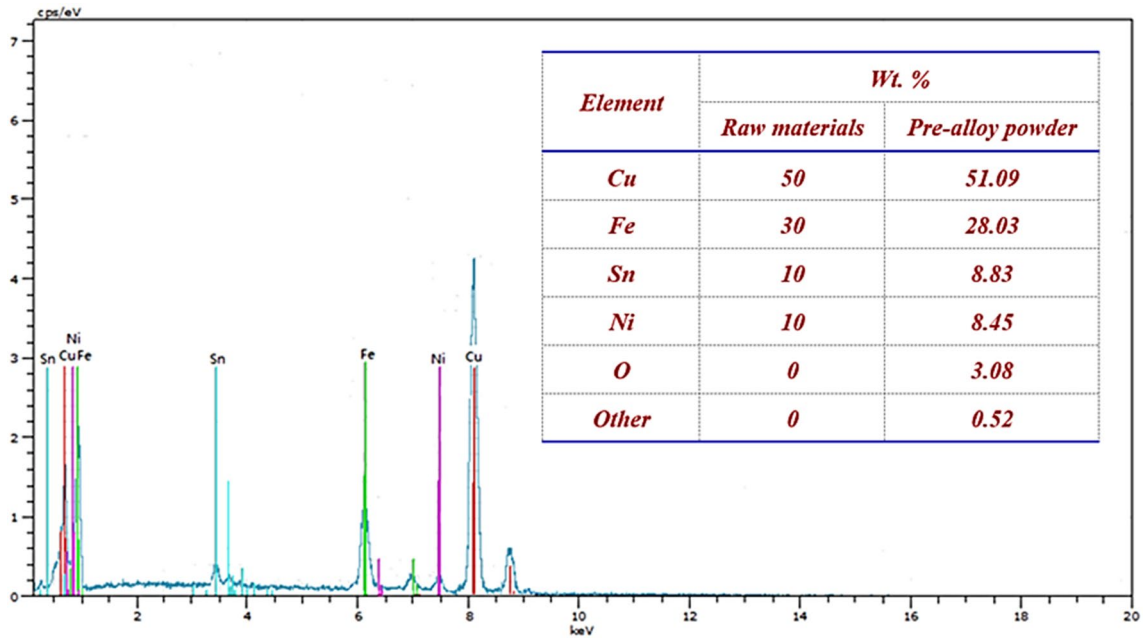

Element	Wt. %	
	Raw materials	Pre-alloy powder
Cu	50	51.09
Fe	30	28.03
Sn	10	8.83
Ni	10	8.45
O	0	3.08
Other	0	0.52

Fig. 5 EDS results of Cu-based pre-alloyed powder

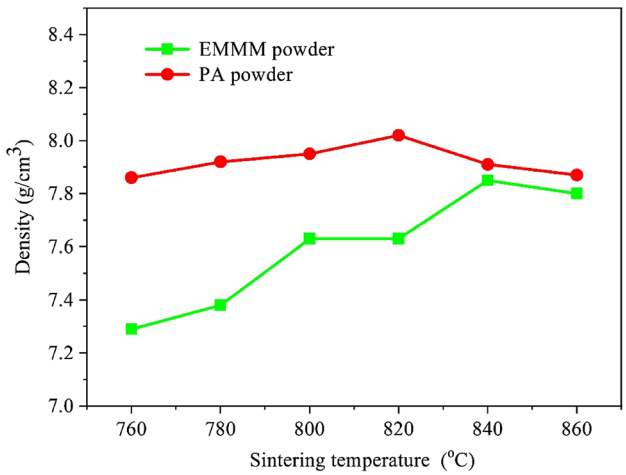

Fig. 6 The density of Cu-matrix bulks

3.3 Properties of Bulks

3.3.1 Density of Bulks

The densities of bulks sintered with PA powder and EMMM powder at different temperatures are compared in Fig. 6. The densities of both bulks increase first and then decrease, and the bulks prepared with PA powder have higher density than the bulks sintered with EMMM powder at the same temperature. The maximum density of the bulk sintered with PA powder is 8.02 g/cm^3 at 820 °C, which is 2.17% higher than the EMMM sample (7.85 g/cm^3 at 840 °C). As the temperature rises, high temperature can promote the growth of ceramic grains and increase the crystallinity, thereby increasing the density of ceramics. However, too high temperatures can lead to excessive sintering of ceramics and even problems such as cracking and deformation (resulting in the irregular shape of the bulks). First, too high temperatures can accelerate the crystallization and growth phenomena in ceramics, causing significant stress on ceramic crystals and having adverse effects on the mechanical properties and density of ceramics. Second, too high temperatures can cause uneven sintering on the surface and interior of ceramics, resulting in inconsistent crystal growth and other issues, thereby damaging the integrity and density of ceramics. In addition, the sintering temperature corresponding to the maximum density reduces by 20 °C. As PA powder has a finer particle size and a large surface area, it has a faster diffusion velocity during sintering, allowing it to transform the hollow surface with high energy into solid crystals with low energy. This results in a significant increase in the sintered bulk density and a reduction in the sintering temperature.

3.3.2 Hardness of Bulks

The hardness values of bulks sintered at different temperatures using EMMM powder and PA powder are displayed in Fig. 7. The hardness of both bulks increases initially before decreasing, in line with the trend of temperature and density variations. The maximum hardness of the bulk sintered with EMMM powder is 100 HRB at 840 °C, while the maximum hardness of the PA sample is 110 HRB at 820 °C, which is

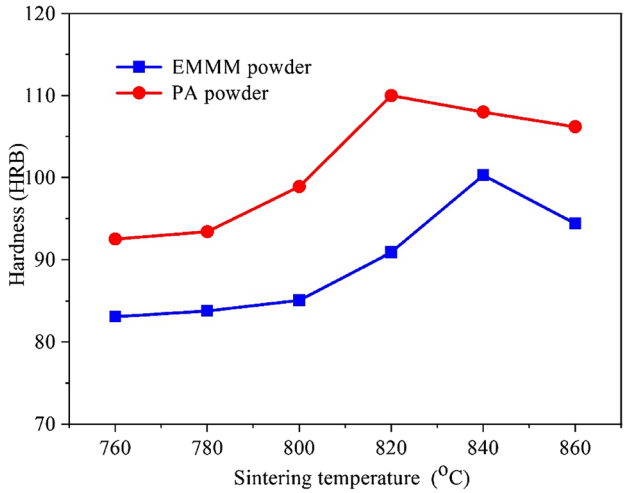

Fig. 7 The hardness of Cu-matrix bulks

10% higher than the EMMM sample. The higher density and finer grain size of PA sample are responsible for the observed results. The hardness of bulks prepared by Cu-based PA powder is higher than that of the bulks prepared by Cu–Fe–Co PA powder using ultra-high-pressure water atomization (98.4 HRB) and conventional water atomization (96.2 HRB) [14].

3.3.3 Flexural Strength of Bulks

The flexural strength of diamond bulks is significantly influenced by the bonding condition at the diamond–matrix interface, and the interface bonding strength of the diamond bulk increases with its flexural strength. Consequently, the interfacial bonding condition can be evaluated by measuring the flexural strength of diamond bulks. The flexural strength results of bulks in the blank matrix and the matrix including diamonds at different temperatures are shown in Fig. 8a, b, respectively. As the temperature of the hot pressing increases, the flexural strength of the bulks experiences an initial rise and a subsequent fall. Similarly, bulks sintered with PA powder have higher flexural strengths than bulks sintered with EMMM powder. As depicted in Fig. 8a, the PA powder sample exhibits a maximum flexural strength value of up to 1056 MPa at 820 °C, which is 21.82% higher than that of EMMM powder sample (846 MPa) at 840 °C. The flexural strength of Cu-based PA powder is higher than that of the bulks prepared by Cu–Fe–Co PA powder using ultra-high-pressure water atomization (964 MPa) and conventional water atomization (940 MPa) [14]. Since the interface between the diamond and matrix is typically the site of fracture, bulks containing diamonds have lower flexural strengths than bulks containing blank matrix [23]. When the diamond particles are added into the PA powder, the maximum flexural strength value of the

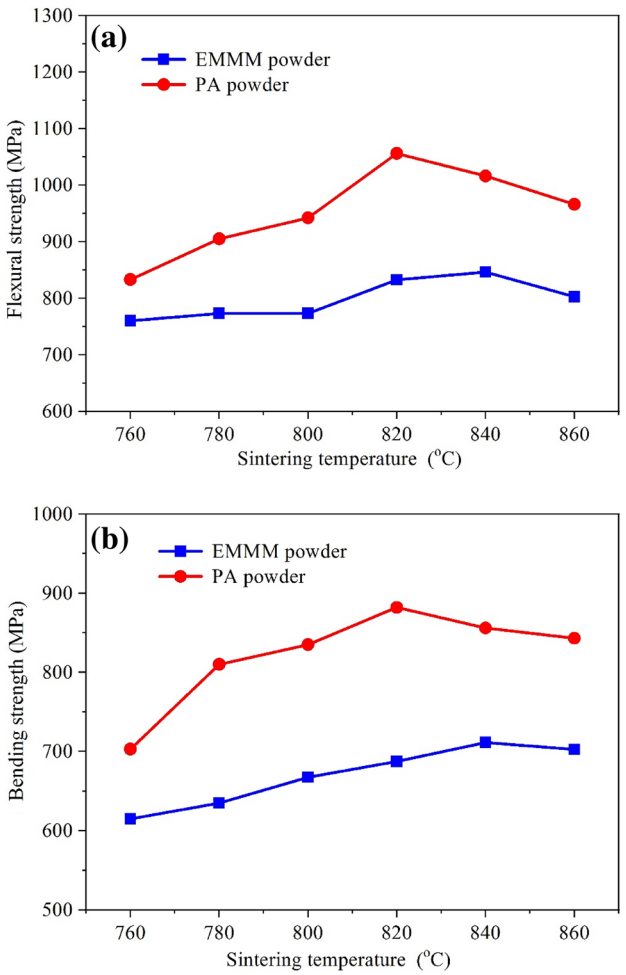

Fig. 8 Flexural strength of the bulks at different temperatures **a** blank matrix, **b** diamond/matrix

bulk is reduced to 856 MPa at 820 ℃ (Fig. 8b). This value is higher than that of the bulks prepared by Cu-Fe-Co PA powder using ultra-high-pressure water atomization (825 MPa) and conventional water atomization (776 MPa) [14]. For the bulk sintered by EMMM powder, the maximal flexural strength value is reduced to 711 MPa at 840 °C, and the value of the bulk made with PA powder is 20.4% greater than that of the EMMM powder bulk. The increase in flexural strength is mainly due to three reasons: (1) the higher density of segments prepared with PA powder compared to EMMM powder; (2) the solid solution strengthening which occurs in PA powder [15]; (3) the grain refining strengthening according to the Hall–Petch relationship [29, 30].

3.4 Fracture Morphology Investigation of Diamond Bulks

The properties of diamond bulks are closely related to the bonding condition between diamond and matrix. The

tighter the bonding between diamond and matrix, the better the properties of diamond bulks. The fracture morphologies of diamond bulks sintered with EMMM powder at 840 °C (Fig. 9a) and PA powder at 820 °C (Fig. 9b) were analyzed. When PA powder is used, the metal matrix is denser and the grain size is smaller. Moreover, the gap between diamond and matrix is narrower, hence enhancing the matrix material's ability to hold diamonds. Comparing the fracture morphologies of diamond bulks sintered with PA powder and EMMM powder, it is evident that PA powder considerably improves the flexural strength.

3.5 Cutting Property of Diamond Saw Blade

In order to test the cutting properties of diamond saw blades made of PA powder and diamond, a diamond tool head was made by sintering PA powder and EMMA powder with diamond, respectively. The diamond saw blade was made by laser welding the diamond tool head to the stainless steel substrate. Diamond saw blades were subjected to the same sintering process as the diamond bulk. The circular diamond saw blade has a U-shaped narrow flume with a diameter of 114 mm, and the diamond tool head has a thickness of 2 mm. The outer and inner hole diameters of the matrix are 90 mm and 20 mm, respectively, and the thickness of the matrix is 1.2 mm.

Granite was utilized as the cutting material in the experiment, with quartz accounting for 40%, plagioclase for 50%, and biotite and other silicate minerals accounting for around 10%. The specific cutting process is as follows: The granite cutting depth is 12 mm, the cutting length is 10 m, the power of the cutting machine is 5.5 kW, and the saw blade speed is 11,000 rpm/min.

The cutting ratio Q was employed in this experiment to correctly assess the cutting performance of the prepared diamond saw blade. Equation (1) was used to determine the cutting ratio:

$$Q = \frac{\triangle m}{S} \tag{1}$$

here, S is the cutting area of the granite, and $\triangle m$ is the weight loss of the saw blade before and after the cutting test ($\triangle m = m_i - m_f$, m_i and m_f are the weights before and after the cutting test).

According to the experimental results, the sawing area of granite is 0.12 m^2, the weight loss of the saw blade made of PA powder is 1.16 g, and that of single metal powder is 2.10 g. According to the calculation, their cutting ratio decreases from 17.5 to 9.67 g/m^2, suggesting that the saw blade's property is improved and its life is extended.

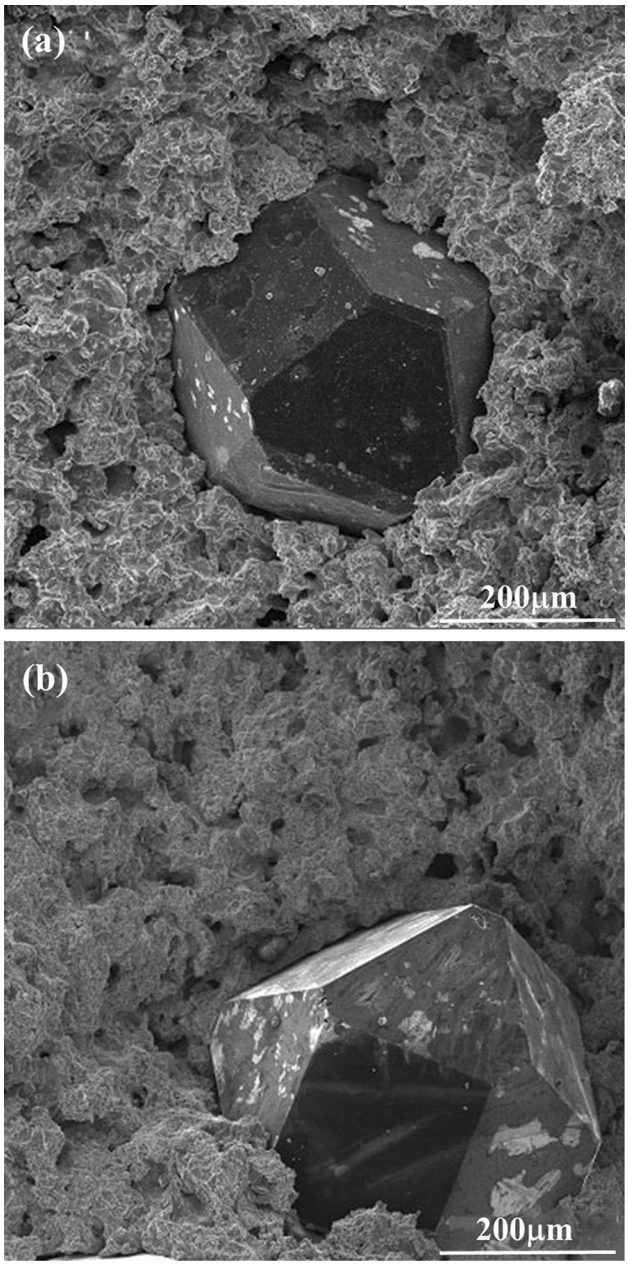

Fig. 9 Fracture morphologies of Cu-matrix bonded diamond bulks with EMMM powder (**a**) and PA powder (**b**)

4 Conclusions

(1) The co-precipitation method is utilized to successfully prepare ultra-fine Cu-based quaternary PA powder. The optimal preparation conditions are: reaction temperature of 50 °C and reactant concentration of 1 mol/L.
(2) The obtained PA powder has an average particle size of 0.55 μm, and its main components are Cu, Fe, Ni, Cu–Sn and Fe_3Ni_2.
(3) Compared to bulks prepared using EMMM powder, those prepared using PA powder have much higher

density, hardness and flexural strength, both with and without diamond particles. Moreover, the corresponding sintering temperature decreases when the properties are optimal. In addition, there is a significant improvement in the mechanical properties of the diamond tools.

(4) The matrix sintered with PA powder exhibits a greater density and a smaller grain size, as well as a narrower gap between the diamond and the matrix.

Funding Changjiang Xiao was received Funding (The key research and development projects of Henan province. Grant No: 231111230500).

References

1. Oliveira L J, Bobrovnitchii G S, and Filgueira M, *Int J Refract Met Hard Mater* **25** (2007) 328.
2. Lin C S, Yang Y L, and Lin S T, *J Mater Process Tech* **201** (2008) 612.
3. Dhokey N B, Utpat K, Gosavi A, and Dhoka P, *Int J Refract Met Hard Mater* **36** (2013) 289.
4. Sun Y X, Tsai Y T, and Lin K H, *Mater Des* **80** (2015) 89.
5. Dai H, Wang L M, Zhang J G, Liu Y B, Wang Y F, Wang L, and Wan X L, *Powder Metall* **58** (2015) 83.
6. Pu J, Sun Y, Long W M, Wu M F, Liu D S, Zhong S J, and Xue S B, *Crystals* **11** (2021) 1427.
7. Barbosa A D P, Bobrovnitchii G S, Skury A L D, Guimaraes R D S, and Filgueira M, *Mater Des* **31** (2010) 522.
8. Chaurasia J J, Ayyapan M, Patel P, Annamalai R, and Rajan A, *Sci Sinter* **49** (2017) 445.
9. Ping H, Xiao F R, Zou W J, and Bo L, *Mater Des* **53** (2014) 38.
10. Xie D L, Wan L, Song D D, Wang S, Lin F, and Pan X Y, *Mater Des* **87** (2015) 482.
11. Shi H C, Duan L C, Tan S C, and Fang X H, *J Alloys Compd* **868** (2021) 159134.
12. Bai R, Zhang S H, Han Y, Zhou H, Su Z, Wang J L, Wu J J, and Liu L L, *Diam Relat Mater* **107** (2020) 107878.
13. Hu H X, Chen W, Deng C, and Yang J D, *J Mater Res Technol* **12** (2021) 150.
14. Chu Z Q, Guo X Y, Liu D H, Tan Y X, Li D, and Tian Q H, *Trans Nonferrous Met Sol China* **26** (2016) 2665.
15. Zhao X J, Li J Y, Duan L C, Tan S C, and Fang X H, *Int J Refract Met Hard Mater* **79** (2019) 115.
16. Dai H, Wang L M, Zhang J G, Liu Y B, Wang Y F, Wang L, and Wan X L, *Powder Technol* **58** (2015) 83.
17. Xu H, Sun S S, Qiao C Y, Feng H Z, Liu Y G, Dong X R, Tao Q, Jiang L N, Zhu P W, and Dong S S, *Diam Relat Mater* **116** (2021) 108439.
18. Clark I E, Kampguis B J, and Cobalite H D R, *Ind Diamond Rev* **62** (2002) 177.
19. Xie D L, Wan L, Song D D, Qin H Q, Pan X Y, and Lin F, *J Wuhan Univ Technol-Mater Sci Ed* **31** (2016) 805.
20. Xie D L, Qin H Q, Lin F, Pan X Y, Chen C, Xiao L Y, Chen J R, and Mo P C, *J Superhard Mater* **41** (2019) 302.
21. Djinovi P, Batista J, Levec J, and Pintar A, *Appl Catal A* **364** (2009) 156.
22. Qiu H J, Huang W W, Zhang Y Q, Chen J, Gao L, Omran M, Nan L, and Chen G, *Ceram Int* **48**(2022) 23452.
23. Pham D H T, Nguyen L T T, Mittova V O, Chau D H, Mittova I Y, Nguyen T A, and Bui V X, *J Mater Sci-Mater E L* **33** (2022) 14356.
24. Vigneswari T, Raji P, and Thiruramanathan P, *T Indian I Metals* **74** (2021) 2255.
25. Pu J, Sun Y B, Long W M, Wu M F, Liu D S, Zhong S J, and Song B X, *Crystals* **11** (2021) 1427.
26. Hu H X, Chen W, and Deng C, *J Mater Res Technol* **12** (2021) 150.
27. Xiao C J, *Surf Eng* **34** (2018) 832.
28. Arulmurugan R, Jeyadevan B, Vaidyanathan G, and Sendhilnathan S, *J Magn Magn Mater* **288** (2005) 470.
29. Petch N J, *J Iron Steel Res Int* **174** (1953) 25.
30. Pande C S, and Cooper K P, *Prog Mater Sci* **54** (2009) 689.